



Scholars Research Library

Archives of Applied Science Research, 2018, 10 (1): 10-16
(<http://www.scholarsresearchlibrary.com>)



ISSN:0975-508X

Remote Control Effect of Li⁺, Na⁺, K⁺ Ions on the Energy Transfer Process in ZnTiO₃:Eu³⁺ Nano-Phosphors Prepared By Combustion Synthesis

Dr. Subhash Chand*

Lecturer at G.H.S. Ballab, Rohtak-124001, Haryana, India

*Corresponding Author: Subhash Chand, Lecturer at G.H.S. Ballab, Rohtak-124001, Haryana, India, Email: DRSCHOPRA78@GMAIL.COM

ABSTRACT

Alkali metal ions (Li⁺, Na⁺ & K⁺) co-doped ZnTiO₃:Eu³⁺ red emitting nano-phosphors series were prepared by combustion synthesis method. The crystal structure & morphology of the prepared phosphors was analyzed by using X-ray diffraction (XRD) and Scanning electron microscopy (SEM). The XRD results show that the crystal structure belongs to the hexagonal phase of ZnTiO₃ with space group R-3:R. From the SEM results, it was observed that the phosphor had very small particle size (10nm-30nm) and the average size of ZnTiO₃ crystal is 30±5nm. PL study showed that under the excitation of UV (393 nm) or blue light (464 nm), the obtained products emitted characteristic red emissions of Eu³⁺ at 615 nm for 5D₀ → 7F₂ transition which proved that activator Eu³⁺ ion had successfully entered the host lattice of ZnTiO₃. The red emission intensity was significantly enhanced by introducing alkali metal ions as co-dopants. A remarkable increase in the photoluminescence intensity is found by co-doping with Li⁺ ions in ZnTiO₃:Eu³⁺ lattices due to the reduction of environment symmetry around Eu³⁺ ions which strengthen the electric dipole transition.

Keywords: Nano composite; Nano electronic devices; Cathode; Tantalum; Ion implantation

Introduction

Luminescence of is especially useful to probe the local structure of luminescent centers in a host lattice because of its simple energy level structure, great sensitivity to ligand field, and similar lanthanide chemical properties to the other rare earth ions [1,2]. Growing interest recently has been focused on luminescence of trivalent rare earth ions in phosphates, tungstates, borates, molybdates, and aluminates, among which rare earth doped borates are especially attractive because of their wide UV transparency, exceptional optical damage thresholds, excellent chemical and thermal stability, and high luminescence efficiency [3-13]. The luminescence study of a series of such compounds provides much valuable information for optical applications. More recently, however, the development of flat panel displays, such as field emission displays (FEDs), plasma display panels (PDPs) and thin film electro-luminescent devices (TFEL), or white light emitting diode (LED), have emerged as the principal motivation for research into rare-earth luminescence, and the present article therefore concentrates on the variety of different ways in which rare-earth luminescence has been exploited in this field [14-17]. White light-emitting diodes (WLED) have attracted more and more attention because of their advantages of environment-friendly, high luminous efficiency, long lifetime and energy-saving [18-19]. One approach has been employed in mixing red, green and blue (RGB) phosphors in an appropriate proportion [20-22]. However, the red phosphor shows lower stability and lower efficiency than the other two [23,24]. Therefore, it is urgent to find new red-emitting phosphors with excellent performance for WLED. Among the rare-earth ions, trivalent europium (Eu³⁺) is an excellent activator for producing red light due to the 5D₀→7F_x (x=0, 1, 2, 3, 4) transitions [25-27]. As a potential inorganic compound, researches on zinc titanate have been mainly focused on its electrical, physical and photo-electrochemical properties, but not much on photoluminescence [28,29]. It was reported by Wang et al. that zinc titanate could be a promising host lattice for luminescent materials [30,31], and in recent years, researches have been focused on improving its luminescence

property [32,33]. Chen et al. reported that when the localized surface plasmon resonance (LSPR) extinction spectrum of Ag nano-particles matched well with the excitation or emission wavelength, the PL intensity of $\text{CaTiO}_3:\text{Eu}^{3+}$ phosphor would be efficiently enhanced by about 1.8 times [34]. Wang et al. reported that the normalized emission intensities of $\text{Sr}_3\text{La}(\text{PO}_4)_3:\text{Eu}^{3+}$ could be distinctly enhanced by about 2.6 times by doping a series of M^+ ($\text{M}=\text{Li}, \text{Na}, \text{K}$) into $\text{Sr}_3\text{La}(\text{PO}_4)_3:\text{Eu}^{3+}$ [35]. Huang et al. studied the effect of alkali metal ions ($\text{Li}^+, \text{Na}^+, \text{K}^+$) on the local structure and luminescence for double tungstate compounds $\text{MEu}(\text{WO}_4)_2$ ($\text{M}=\text{Li}, \text{Na}, \text{K}$) prepared by a dual-space arches, indicating that the alkali metal ions could lead to some positive effects [36]. Some ions may enter into the host lattice, and the others could act as sensitizer or flux, bringing about oxygen vacancies or changing the crystal field surrounding the activator, and then influencing the photoluminescence performance [37-39]. As we know, every synthesis methods have some important effects on structure and physical properties of material. Here we applied the combustion synthesis [40] for the preparation of europium doped Zn titanates phosphors which involve fast & thermal decomposition of the rare earth nitrate in the presence of an organic fuel. During the combustion, many gases like $\text{CO}_2, \text{N}_2, \text{NO}_2$ etc as well as a large amount of heat are released with in a short period of time thus resulting in a white, fluffy phosphor. This method has been utilized with the aim to prepare nano-sized crystalline powders of ZnTiO_3 doped with Eu^{3+} and co-doped with charge compensators like especially mono-valent cations after sintering at 1000 °C. Here the effect of addition of monovalent ions like Li^+, Na^+ and K^+ etc into ZnTiO_3 lattices to enhance the luminescence intensity had been studied and the possible mechanism has been proposed. The crystal structure, morphology and PL properties of the phosphor thus synthesized are characterized by X-ray diffraction technique, Scanning electron microscope (SEM) and PL spectra obtained by using an under the excitation of UV (393 nm) or blue light (464 nm). In this work, we are reporting a significant enhancement in red emission intensity of $\text{ZnTiO}_3:\text{Eu}^{3+}$ nano-phosphor by introducing alkali metal ions as co-dopants. Hence the influences of addition of alkali metal ions on the energy transfer process and also on luminescence intensity is discussed in detail and the most suitable one has been determined.

EXPERIMENTAL PROCEDURES

Synthesis of $\text{ZnTiO}_3:\text{Eu}^{3+}, \text{M}^+$ ($\text{M}^+=\text{Li}, \text{Na}, \text{K}$) nano phosphors:

Stoichiometric amounts of highly purified (99.9%) TiO_2 [1.0 mole], $[\text{Zn}(\text{NO}_3)_2]$, $[\text{Eu}(\text{NO}_3)_3]$, $[\text{LiNO}_3]$, $[\text{NaNO}_3]$, $[\text{KNO}_3]$ and Urea as a combustion fuel were used for the preparation of Eu^{3+} doped ZnTiO_3 and M^+ co-doped $\text{ZnTiO}_3:\text{Eu}^{3+}, \text{M}^+$ nano-crystals ($\text{M}^+=\text{Li}^+, \text{Na}^+, \text{K}^+$) with general formula $\text{Zn}_{(1-x)}\text{TiO}_3:\text{Eu}^{3+}$ and $\text{Zn}_{(1-x-y)}\text{TiO}_3:\text{Eu}^{3+}, \text{M}^+$ where x is 0.5 to 3 mol% & y is 1 to 6 mol%. By heating a stoichiometric amount of above said materials on a preheated hot plate maintained at 150°C & the white solid thus obtained further calcined in muffle furnace at 1000 °C for 3 h to enhance the crystallinity of the phosphor.

Characterization of the phosphor:

White solid grounded to fine sized powder by the pestle mortar was characterized by X-ray diffraction, Scanning electron microscopy (SEM) & PL measurement to determine the crystallinity, particles size & luminescence intensity respectively. All measurements were carried out at room temperature.

RESULTS AND DISCUSSION

Crystal structure analysis

The crystal structure and phase purity were examined by X-ray diffraction patterns of ZnTiO_3 phosphors are shown in Figure 1. It can be clearly indicated by all diffraction peaks of the samples match well with that of hexagonal-phase ZnTiO_3 (JCPDS- No. 26-1500), indicating that Eu^{3+} and M^+ ($\text{M}^+=\text{Li}^+, \text{Na}^+, \text{K}^+$) were incorporated into the lattice successfully and co-doping of different kinds of alkali metal ion have not led to the formation of other phases.

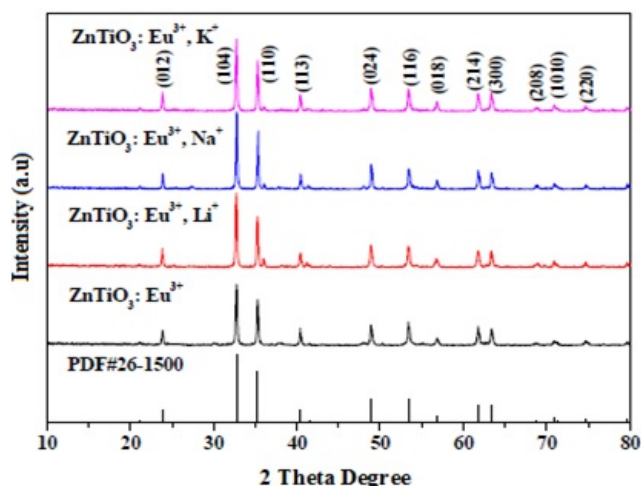


Figure 1: XRD pattern of $\text{ZnTiO}_3:\text{Eu}^{3+}$ and M^+ ($\text{M}=\text{Li}, \text{Na}, \text{K}$) calcined at 1000 C for 3 h.

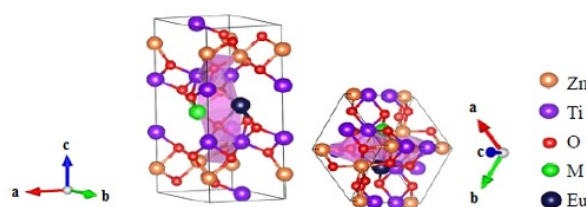
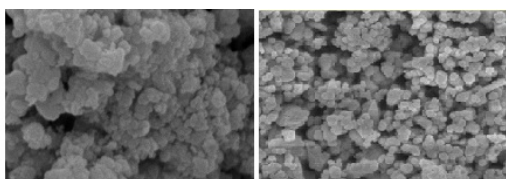


Figure 2: Crystal structure of hexagonal ZnTiO_3 and schematic diagram of the substitution by Eu^{3+}/M .

The structure of hexagonal ZnTiO_3 can be further well described by space group $R\bar{3}R$ with lattice constants $a=b=5.0787$, $c=13.927$ Å. As shown in Figure 2, it is observed that two Zn^{2+} ion may be replaced by one Eu^{3+} and one M^+ ion so as to get charge balance, but the experimental results are more complicated.

SEM micrograph and particle size analysis

The photoluminescence is strongly affected by the crystallinity, particle size and surface roughness of the phosphor. Figure 3 (a) & (b) show the SEM images of the $\text{ZnTiO}_3:\text{Eu}^{3+}$ and Li-doped $\text{ZnTiO}_3:\text{Eu}^{3+}$ nano-particles which also support the hexagonal structures of $\text{ZnTiO}_3:\text{Eu}^{3+}$ and Li^+ co-doped $\text{ZnTiO}_3:\text{Eu}^{3+}$. The particle show good uniformity, smooth and dense microstructures with sizes range around 1030 nm.



(a) 30nm (b) 10nm

Figure 3: SEM images of (a): $\text{ZnTiO}_3:\text{Eu}^{3+}$ and (b): $\text{ZnTiO}_3:\text{Eu}^{3+}, \text{Li}^+$ phosphors.

Luminescent properties

Figures 4 and 5 depict the excitation and emission spectra of samples $\text{ZnTiO}_3:\text{Eu}^{3+}$ and M^+ ($\text{M}^+=\text{Li}^+, \text{Na}^+, \text{K}^+$). It can be clearly seen that their regular patterns and peak positions of each curve are almost similar except intensity. The result indicates that the incorporation of alkali metal ions into $\text{ZnTiO}_3:\text{Eu}^{3+}$ leads to little effect on the splitting of Eu^{3+} and energy level shift [41]. Figure 4 depicts the excitation spectra of samples monitored at 615 nm. The broad bands from 250 to 350 nm are mainly attributed to charge transfer (CT) transition from O^{2-} to Eu^{3+} [42]. The excitation peak located at 464 nm is assigned to the $7F_0 \rightarrow 5D_2$ transition, and less intense absorption at 393, 385 and 414 nm is assigned to $7F_0 \rightarrow 5L_6$, $7F_0 \rightarrow 5L_7$ and $7F_0 \rightarrow 5D_3$, respectively [43]. As indicated in Figure 5, the emission

intensities of $\text{ZnTiO}_3:\text{Eu}^{3+}$, M^+ ($\text{M}^+=\text{Li}^+$, Na^+ , K^+) are found to be stronger than that of $\text{ZnTiO}_3:\text{Eu}^{3+}$ phosphors. Thus, the relative intensity of the emission spectrum of Li^+ , Na^+ and K^+ co-doped samples is increased by 1.63, 1.41 and 1.22 when compared to that of $99.08\text{ZnTiO}_3:0.02\text{Eu}^{3+}$. It indicates that the incorporation of alkali metal ions (Li^+ , Na^+ , K^+) can effectively enhance the luminescence intensity of the $\text{ZnTiO}_3:\text{Eu}^{3+}$ phosphor. This phenomenon can be probably contributed to the fact that the effective ionic radius of Li^+ ion ($R_{\text{Li}^+}=59$ pm, $R_{\text{Na}^+}=99$ pm & $R_{\text{K}^+}=137$ pm) is almost the same as that of Zn^{2+} ($R_{\text{Zn}^{2+}}=60$ pm) and the Zn^{2+} can be easily replaced by Li^+ [44].

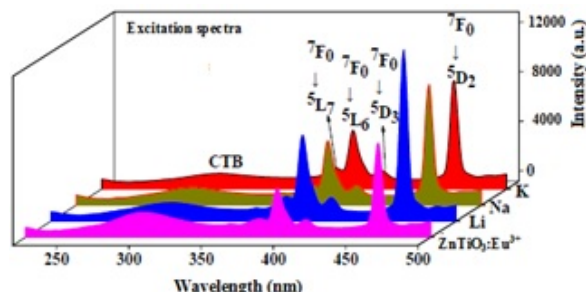


Figure 4: Excitation spectra of $\text{ZnTiO}_3:2\%\text{Eu}^{3+}$ & $2\%\text{M}^+=\text{Li}$, Na , K ($\lambda_{\text{em}}=615$ nm).

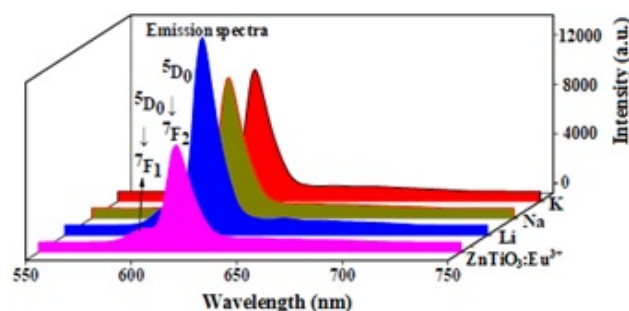


Figure 5: Emission spectra of $\text{ZnTiO}_3:2\%\text{Eu}^{3+}$ & $2\%\text{M}^+=\text{Li}$, Na , K ($\lambda_{\text{ex}}=464$ nm).

Therefore, this substitution in the lattice induced fast energy transfer from the host to the Eu^{3+} ion, and hence created an increase in the hole concentration leading to a decrease in competitive absorption, as a result to a higher quantum yield [45]. According to Dexter's theory [46], the multipolar interaction occurring between the same activators can be calculated by formula (1) given below:

Where, K and L are constants for the given host, x is the activator concentration, and Q is the constant of multipolar interaction and equals to 10, 8, 6 for quadrupole - quadrupole (q-q), dipole-quadrupole (d-q) and dipole-dipole (d-d) interactions, respectively. Figure 6 shows the relation between $\log(I/x)$ and $\log(x)$ $\text{ZnTiO}_3:\text{Eu}^{3+}$ phosphor under the Eu^{3+} concentration of 1%, 1.5%, 2%, 2.5%. The slope of the curve is found to be -1.96 . The value of Q is calculated to be 5.89 which is close to 6, suggesting that dipole-dipole (d-d) interaction is the main mechanism for the concentration quenching [47] between Eu^{3+} ions and the $\text{ZnTiO}_3:\text{Eu}^{3+}$ phosphor. The emission intensities of $\text{ZnTiO}_3:\text{Eu}^{3+}$, M^+ phosphors are given in Figure 7. The results show that the emission intensity increases with increasing the M^+ concentration at first, and then decreases when it reaches a maximum value of 4 mol%. When the content of alkali metal ions is less than 2 mol%, the emission intensity can be improved because Eu^{3+} can partially substitute Zn^{2+} , and then offset unbalanced charge between Eu^{3+} and Zn^{2+} [43]. When the content of alkali metal ions is more than 2 mol% and less than 4 mol%, the luminous intensity of samples is further improved.

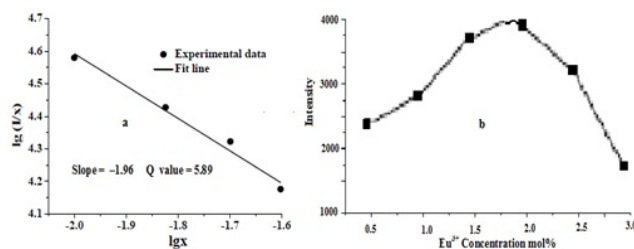


Figure 6: (a) Plot of $\lg(I/x)$ as a function of $\lg(x)$ & (b) Intensity v/s in Eu^{3+} mol% concentration in $\text{ZnTiO}_3:\text{Eu}^{3+}, \text{M}^+$ phosphors ($\lambda_{\text{ex}}=464$ nm).

It is considered as the energy transfer enhanced between the substrate (ZnTiO_3) and activator (Eu^{3+}) with the alkali metal ions concentration increasing. However, when the content of alkali metal ions is higher than 4 mol%, the host lattice integrity will be destroyed. As a consequence, ZnTiO_3 phosphor luminescence intensity decreases. Moreover, it is considered that the ions ($\text{Li}^+, \text{Na}^+, \text{K}^+$) substituting for Zn^{2+} could create point defects such as oxygen vacancies. The differences in charge number and radius values between alkali metal ions, Eu^{3+} and Zn^{2+} , will cause the formation of bond electron-hole pair and change the Eu-O distance slightly [48]. The different alkali metal ions can bring different degree of impacts. Therefore, the relative intensities of excitation and emission for $\text{ZnTiO}_3:\text{Eu}^{3+}, \text{M}^+$ are different.

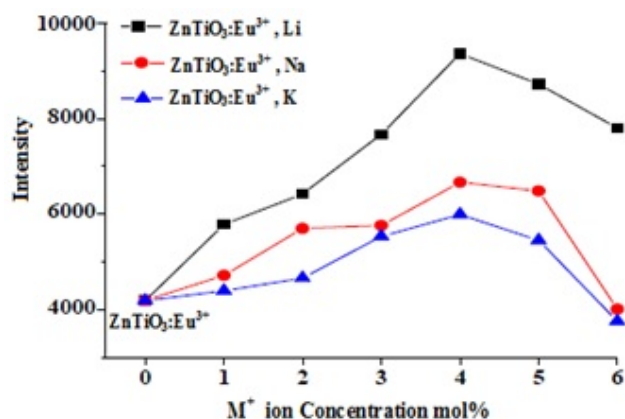


Figure 7: Normalized intensities of $\text{ZnTiO}_3:\text{Eu}^{3+}, \text{M}^+$ [$\text{M}^+=\text{Li}, \text{Na}, \text{K}$] conc. ($\lambda_{\text{ex}}=464$ nm)

Chromaticity co-ordinates analysis

CIE 1931 chromaticity coordinates of $\text{ZnTiO}_3:\text{Eu}^{3+}$ and $\text{ZnTiO}_3:2\%\text{Eu}^{3+}, 4\% \text{Li}^+$, and the National Television Standard Committee (NTSC) standard for red and $\text{Y}_2\text{O}_2\text{S}:\text{Eu}^{3+}$ are shown in Figure 8, which are calculated by the CIE 1931 color matching functions[49].

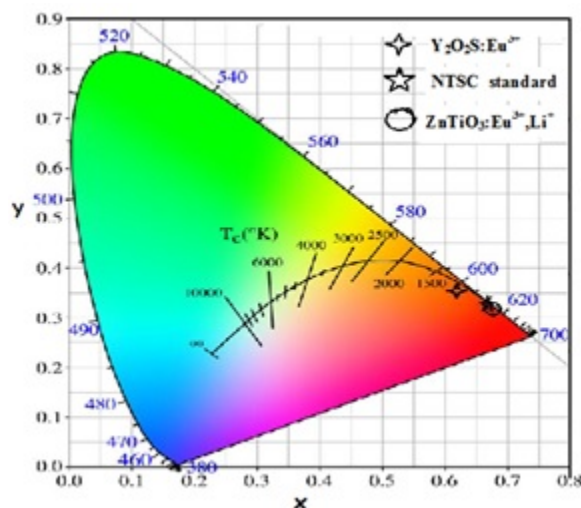


Figure 8: CIE 1931 chromaticity coordinates of $\text{ZnTiO}_3:\text{Eu}^{3+}$ and $\text{ZnTiO}_3:\text{Eu}^{3+},\text{M}^+$ ($\text{M}=\text{Li}$).

The calculated value for CIE coordinates for $\text{ZnTiO}_3:2\%\text{Eu}^{3+}$, 4% Li^+ are found to be $x=0.672$ and $y=0.329$, similar to the standard red color (0.670, 0.330) in the NTSC system.

CONCLUSION

A series of $\text{ZnTiO}_3:\text{Eu}^{3+}$, M^+ ($\text{M}^+=\text{Li}$, Na, K) red emitting nano-phosphors was successfully synthesized by combustion method. The XRD and SEM results show that ZnTiO_3 nano-particles exhibit a hexagonal phase with particle sizes range around 10 to 30 nm. When phosphors excited by UV (393 nm) or blue light (464 nm) emitting intense- red light at the peak of 615nm. The PL intensity is optimized by co-doping of some alkali metal ion concentration of 4 mol%. When co-doping 4 mol% Li^+ , Na^+ , and K^+ into $\text{ZnTiO}_3:2\%\text{Eu}^{3+}$, the normalized intensity of $\text{ZnTiO}_3:2\%\text{Eu}^{3+}$ is increased by 2.1, 1.7 and 1.4 times compared with $\text{ZnTiO}_3:2\%\text{Eu}^{3+}$. The CIE chromaticity coordinates of the $\text{ZnTiO}_3:2\%\text{Eu}^{3+}$, Li^+ phosphors are similar to the National Television Standard Committee (NTSC) standard CIE chromaticity coordinate values for red (0.670, 0.330). These results show that $\text{ZnTiO}_3:\text{Eu}^{3+}$, M^+ red-emitting phosphors can be applied in high quality WLED potentially.

REFERENCE

1. Zhang X M and Seo H J, *J Alloys Compd.*, **2011**, 509; p.2007–2010.
2. Pires A M, Santos M F, et al, *J Alloys Compd*, **2002**, 344 (1-2); p.276–279.
3. Driesen K, Tikhomirov V K, et al, *J Appl Phys.*, **2007**, 102; Article ID 024312.
4. Yan C. H, Sun L D, et al, *Appl Phys Lett.*, **2003**, 82(20); p.3511–3513.
5. Stefani R, Maia A D, et al, *J Solid State Chem.*, **2006**, 179 (4); p.1086–1092.
6. Won Y, Jang H, et al, *J Electrochem Soc.*, **2008**, 155(9); p.J226–J229.
7. Ayvacıklı M, Ege A, et al, *Opt Mater.*, **2011**, 34(1); p.138–142.
8. Yang Y M, Ren Z Y, et al, *Curr Appl Phys*, **2009**, 9; p.618–621.
9. Tu D, Liang Y J, et al, *J Alloys Compd*, **2011**, 509(18); p.5596–5599.
10. Hao J H, Gao J, et al, *Appl Phys Lett*, **2003**, 82 (17); p.778–2780.
11. Henkes A E and Schaak R E, *J Solid State Chem*, **2008**, 181(12); p.3264–3268.
12. Ju G. F., Hu Y. H, et al, *Opt Mater*, **2011**, 33; p.1297–1301.
13. Yang J, and Zhang C M, et al, *Inorg Chem.*, **2008**, 47 (16); p.7262–7270.
14. Duan C, Yuan J, et al, *J Phys D: Appl Phys.*, **2005**, 38; p.3576.
15. Komeno A, Uematsu K, et al, *J Alloys Compd.*, **2006**, 871; p.408–412 .
16. Kitai A H, *Thin Solid Films.*, **2003**, 445; p.367.
17. Sivakumar V and Vardaraju U V, *J Electrochem Soc.*, **2005**, 152 (10); p.H168.
18. Pimpitkar S, Speck J S, et al, *S Nat Photonics.*, **2009**, 3; p.180–182.

19. Ogi T, Nandiyanto, et al, *Chem Eng J.* , **2012**, 210; p.461–466.
20. Zhang X G, Zhou L Y, et al, *Opt Mater.*, **2013**, 35; p.993–997.
21. Haque M M, Lee H I, et al, *J Alloy Compd.* , **2009**, 481; p.792–796.
22. Chen Y B, Cheah K W, et al, *J Lumin.*, **2011**, 131; p.1770–1775.
23. Yang H M, Shi J X, et al, *J Alloy Compd.*, 2006, 415; p.213–215
24. Herrmann A, Simon A, et al, *C J Lumin.*, **2012**, 132; p.215–219.
25. Yuan T S, Zhou H T, et al, *J Struc Chem.*, **2010**, 29; p.919–925.
26. Zadlo M, Sroka B S, et al, *J Rare Earth*, **2014**, 32; p.269–272.
27. Song H J, Zhou L Q, et al, *J Struc Chem.*, **2013**, 26; p.83–87.
28. Fu J., Zhang Q. et al, *J Lumin.* , **2010**, 130; p.231–235.
29. Ye S, Xiao F, et al, *Mater. Sci. Eng.*, **2010**, 71; p.1–34.
30. Wang S F, Lv M K, et al, *Inor. Chem. Commu.*, **2003**, 6; p.185–188.
31. Wang S F, Gu F, et al, *Chem. Phys. Lett.*, **2003**, 373; p.223–227.
32. Li M T, Jiao, et al, *J. Rare Earth* , **2015**, 33; p.231–238.
33. Yao S S, Xue L H, et al, *Curr. App. Phys.*, **2011**, 11; p.639–642.
34. Balasanthiran C, Zhao B, et al, *J. Colloid. Interf. Sci.*, **2015**, 459; p.63–69.
35. Wang Z, Lou S, et al, *J. Alloy. Compd.*, **2016**, 813–817.
36. Huang J, Xu J, et al, *Inorg. Chem.*, **2011**, 50; p.11487–11492.
37. Liang H B, Zhang G B, et al, *J. Lumin.*, **2011**, 131; p.194–198.
38. Yi S S, Bae J S, et al, *Appl. Phys. Lett.*, **2004**, 84(8); p.353–355.
39. Yang D, Li G, et al, *Nano-scale* , **2012**, 4, 3450–3459.
40. Ekambaram S and Patil K C, *J. Alloys Compd.*, **1997**, 7; p.248.
41. Liu X, Han K, et al, *Solid State Commun.*, **2007**, 142; p.680–684.
42. Wang Z, Li P, et al, *J. Lumin.*, **2012**, 132; p.1944–1948.
43. Kominami H, Tanaka M, et al, *Phys. Status Solidi (c)*, **2006**, 3; p.2758–2761.
44. Mu Z, Hu Y, et al, *Opt. Mater.*, **2011**, 34; p.89–94.
45. Lin C K, Kong D Y, et al, *J. Inorg. Chem.*, **2007**, 46; p.2674–2681.
46. Jia P Y, Liu X M, et al, *J. Chem. Phys. Lett.*, **2006**, 424; p.358–363.
47. Ilhan M, Samur R, et al, *Metalurgija.*, **2015**, 54(2); p.407–410
48. Li L L, Liu L, et al, *J. Lumin.*, **2013**, 143, p.14–20.
49. Yang M Z, Sui Y, et al, *Chem. Phys. Lett.*, **2010**, 492; p.40–43.